# Per-Pixel Radiometric Calibration of Camera Images from an LCD Monitor

Tobias Elbrandt, Jörn Ostermann
Institut für Informationsverarbeitung
Leibniz Universität Hannover
Hannover, Germany
elbrandt@tnt.uni-hannover.de

*Abstract*—This paper presents a method to calibrate the radiometric response function for every single pixel of a camera capturing grayscale images from an LCD monitor. Captured images from all available brightness levels of the monitor are used to estimate the parameters of scaled biased exponential functions for every pixel. The inverses of the estimated functions are then used to calibrate camera pictures. Our method restricts the average overall error of about 0.45% of brightness or an SNR of 40.17 dB for the whole camera target and all brightness levels. These results prove that our method permits the usage of continuous-tone monitor images for camera calibration.

***Keywords-Camera, Calibration, Radiometry.***

## I. INTRODUCTION

Radiometric calibration in the context of cameras is the determination of the response function of the output signal for a given amount of light. Especially in the fields of high dynamic range imaging and image stitching, the radiometric calibration is a highly active research field. [1] presented a method to estimate the response function from gradients within a single gray-scale image. [2] use correspondent points from a few different images taken from a scene. The inherent statistical properties of a digital camera were analyzed in [3].

All of the above mentioned works assume one camera-specific response function that is constant for all pixels of the camera target. In particular they do not take into account different functions for different color channels due to Bayer color mosaicing but work with gray or demosaiced color images.

Some methods like [4] and [5] measure the camera's distortion by capturing black-and-white calibration patterns displayed on a monitor. This approach offers controlled laboratory conditions concerning the setup which guarantees reproducible and accurate measurements. However, the calibration accuracy is limited by aliasing and unsharpness, which can be overcome by using continuous-tone patterns. That in turn requires a per-pixel radiometric calibration of the camera. Our work presented here provides this calibration and therefore solves the aforementioned problems.

The relation between the brightness displayed on the screen and the light intensity measured by an element of the camera target is mainly influenced by the following factors (the last four effects are additional influences due to the utilization of a monitor):

- **brightness** of the displayed pattern;
- **gamma** of the used camera[1];
- different sensitivity of the elements of the camera target because of a **color filter mosaic**;
- different sources of **camera noise**, and **quantization**;
- increasing **distance** between the lens and the monitor surface leads to an attenuation of light intensity and geometric spreading;
- **gamma** of the used monitor;
- for each pixel of the monitor there is an unbiased **noise** affecting the actually displayed brightness;
- **angle** of view; the angle is 0° where the optical axis of the camera meets the screen surface – provided the camera is positioned orthogonal to the display – and e.g. 30° in the corners of the camera target – depending on the type of lens;
- **aliasing** due to rasterization of both LCD elements and camera target sensitive elements.

The next section describes our approach for the camera calibration addressing all of the above mentioned effects. Section III describes experiments and analyzes them. Section IV assesses the overall results. The last section concludes our work.

## II. PER-PIXEL RADIOMETRIC CALIBRATION

The radiometric calibration procedure displays calibration patterns on the LCD monitor and captures them with the camera to determine the relation between the brightness displayed on the monitor and the measured light intensity on the camera target.

We determine this relation separately for every camera element which avoids the influences of angle dependent irradiance, distance dependent optical loss, and aliasing effects, since these are constant within one

[1] Normally the output voltage of a CCD element is proportional to the number of perceived light quantums but some cameras adjust the output signal to achieve better images for the human eye. The resulting response function is usually similar to a gamma curve [6].

camera pixel. Different sensitivity levels of the camera target elements behind the Bayer color filter mosaic are also neglected using the raw pixel data instead of already demosaiced full-color pictures. The interference of the unbiased noise sources (shot noise, read noise, and quantization) is decreased by averaging multiple camera images of the same pattern, whereas the dark current noise and fixed pattern noise give a certain bias [3].

Both gamma functions of monitor $f_m$ and camera $f_c$ can be easily combined as

$$f_c(f_m(x)) = \lambda_c(\lambda_m x^{\gamma_m})^{\gamma_c} = \lambda x^{\gamma} \quad (1)$$

$$\text{with } \lambda = \lambda_c \lambda_m^{\gamma_c} \text{ and } \gamma = \gamma_c \gamma_m$$

The only parameters left to describe the relation between the brightness of the displayed pattern and the perceived light intensity in the camera elements are the combined gamma $\gamma$, a certain linear factor $\lambda$, and the bias $\beta$. Therefore, it is reasonable to describe the relation as a biased scaled exponential function

$$I(b) = \lambda b^{\gamma} + \beta \quad (2)$$

where $b$ is the displayed brightness, $I$ is the measured intensity, and $\lambda$, $\gamma$, and $\beta$ are the parameters to estimate.

### A. Measuring the Response Function

The camera is positioned in front of the LCD monitor such that its optical axis is reasonably orthogonal to the center of the screen surface. It is positioned as closely as necessary to map only screen pixels onto the camera target – no camera pixel should capture light coming from a different place than the monitor surface. Due to unsharpness and not corresponding grids of camera and monitor, every camera pixel captures a portion of several monitor pixels at the same time. The brightness level of the monitor and the shutter/exposure time of the camera are adjusted such that clipping of the signal is prevented.

Screens with all pixels set to gray with same brightness level $b$ are displayed on the monitor and captured $N$ times as measurements $\hat{C}_{b,i}(x,y) \in [0..255]$, $i = 1..N$, $0 \le x < w_c$, $0 \le y < h_c$. The constants $w_c$ and $h_c$ denote the width and height of the camera target, respectively, and the perceived light intensities are quantized to 256 levels. The captured images are then averaged to

$$\hat{I}_b(x,y) = \frac{1}{N}\sum_{i=1}^{N} \hat{C}_{b,i}(x,y) \quad (3)$$

This is done for all available 256 intensity levels of $b$.

### B. Calculation of the Calibration Parameters

The parameters $\lambda$, $\gamma$, and $\beta$ of Eq. (2) have to be determined independently for every single pixel $(x, y)$ of the captured and averaged images $\hat{I}_b$. This is done by taking the measured intensity values at the same pixel $(x,y)$ from all 256 images, i.e. $\hat{I}_b(x,y)$, $b=0..255$, with $x$, $y$ fixed, and calculating a biased power regression. As the power regression itself is only able to estimate the parameters of $f(x) = \lambda x^{\gamma}$, i.e. without bias $\beta$, we have to estimate the bias numerically. For this purpose, we define an error function $\varepsilon_I$ to minimize as

$$\varepsilon_I(\beta) = \sum_{b=0}^{255} \left(I(b) - \hat{I}_b\right)^2 \quad (4)$$

For any given $\beta$, the parameters $\lambda$ and $\gamma$ are estimated with a linear regression for the data points ( log(b), $\log(\hat{I}_b - \beta)$ ) where all data points with $\hat{I}_b < \beta + \varepsilon$ are skipped because their absolute logarithm is too large or undefined. This causes the error function to be discontinuous at these points. The bias $\beta$ minimizing the error function is chosen; for each point $(x,y)$ the parameter set $\{\lambda, \gamma, \beta\}$ is found.

### C. Calibration

Given the set of parameters, the perceived light intensity at each pixel position $(x,y)$ can be calibrated. As Eq. (2) gives the relation $I(b) = i$ between displayed brightness $b$ and perceived intensity $i$, we need the inverse function $I^{-1}(i) = b$ for the radiometric calibration to determine which brightness level $b$ was displayed when an intensity level $i$ was perceived. It is derived as

$$I^{-1}(i) = \left(\frac{i-\beta}{\lambda}\right)^{\frac{1}{\gamma}} \quad (5)$$

Given a captured image, the brightness value $b$ of each pixel $(x,y)$ for the calibrated image can be calculated with Eq. (5) and the parameter set $\{\lambda, \gamma, \beta\}$ for that pixel.

## III. EXPERIMENTS

Our setup consists of a Prosilica EC 1380C FireWire camera with Schneider-Kreuznach Cinegon 1.4/8-0512 industrial lens and a Samsung 910 T 19" TFT monitor. The camera was arranged in front of the monitor as described above with a distance of approximately 30cm. Its view span about 1200 × 900 monitor pixels. The gamma of the monitor or graphics card was not adjusted in the first step.

The white balance was set while capturing a checkerboard pattern. Brightness and shutter time were set to values such that no output intensity level exceeded 200. This restriction was necessary to handle the nonlinear modification of the green pixels at higher brightness levels of our camera.

We displayed each of the 256 images with increasing brightness on the monitor and captured it 16 times with the full camera resolution of 1360 × 1024 pixel. The upper left quarter of the averaged images with brightness 255 is shown in Fig. 1. As the sensitivity to light of the pixels behind the Bayer color mosaic differs between the colors, the raw image cannot be printed accurately. Therefore, only the intensity of the red channel is shown.

It is mainly observed that the perceived light intensity decreases with increasing viewing angle. Whereas the pixels shown in the lower right corner of Fig. 1 are viewed directly by the camera, the pixels shown in the

upper left corner are viewed under an angle of about 30°; the intensity value decreases from 190 to 35.


Figure 1. Upper left quarter of the red channel of the captured image when the monitor displayed only white pixels.

For every pixel of the averaged images, the power regression parameters $\lambda$, $\gamma$, and $\beta$ were calculated. The respective average gamma parameters for red, green, and blue (1.951, 1.927, and 1.767) are used to adjust the gamma value of the monitor, i.e. the graphics card is set to these values.

After adjusting the monitor gamma, we started a second measurement with displaying the 256 brightness levels on the monitor. Again, a biased power regression is calculated for every position of the camera target.

Fig. 2 shows an example for the error function $\varepsilon_I$ at pixel position (400, 400) for bias values from $\beta = 0.0$ to $\beta = 2.5$. At this position, the chosen optimal parameters were $\lambda = 0.384205$, $\gamma = 1.025406$, and $\beta = 1.461847$. Please note that the discontinuity at the values of $\hat{I}_b$ are not necessarily at integer numbers since they were determined as the average of N pixel intensities.

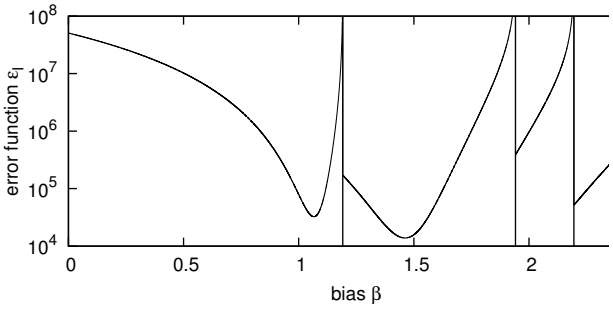


Figure 2. Error function $\varepsilon_I$ over bias $\beta$ at pixel (400,400). It is discontinuous at the values of the intensity values $\hat{I}_b$.

The calculated calibration parameters for the pixels corresponding to Fig. 1, i.e. the red channel pixels of the upper left quarter, are shown in Fig. 3 a), b), and c). One cannot actually identify an individual parameter set from these images but one can recognize some characteristics of them:

Each of the parameters shows a certain trend from the center of the image (lower right corner) to the edge, but in between it is not distributed uniformly. In both the gradient and gamma images significant local variations in addition to some noise can be detected. The latter comes from the algorithm estimating the parameters which is very prone to noisy input data, but the local variations indicate that a per-pixel calibration is absolutely necessary.

## IV. RESULTS

The estimated calibration parameters can now be applied to the pictures previously captured by the camera. Comparing the brightness value $b$ initially displayed on the monitor, i.e. ground truth, with a new set of captured images $\hat{I}_b$ calibrated with the determined $I^{-1}()$ functions gives a measure for the accuracy of the calibration.

The mean error between ground truth and calibrated intensity level and the respective standard deviation over the whole image are shown in Fig. 4 a) for all brightness levels. One can see that the mean error is unbiased while the standard deviation grows with increasing brightness level. The overall errors (mean ± 1.5 and standard deviation 2.5) are quite small compared to the overall range of 256 brightness levels, which can be seen in Fig. 4 b). Obviously, the relative errors for monitor brightness values below 4 are higher than 0.1.

The overall errors are summed up in Table I. For a respective brightness level $b$ the SNR (Signal-to-Noise Ratio) was calculated with $SNR_b = 10 \log_{10}( b^2 / MSE_b )$ whereas the mean SNR was calculated with $10 \cdot \log_{10} \left( \frac{1}{255} \sum_{b=1}^{255} \frac{b^2}{MSE_b} \right)$. In relation to the absolute signal amplitude of 255 levels, the mean and maximum absolute errors correspond to relative errors of 0.45% and 1.04%, respectively.

To clarify the quality of these results, we calculate the error which is only caused by quantization with the following equation:

$$MSE_b = \frac{1}{w_c h_c} \sum_{x,y} \left( b - I_{x,y}^{-1} \left( \left\lfloor I_{x,y}(b) + 0.5 \right\rfloor \right) \right)^2 \qquad (6)$$

All ground truth values are transformed, quantized and inverse transformed. The mean squared error results in an SNR of 43.37 dB, which means, that the major part of the error of our calibration algorithm is caused by the inherent quantization. This shows that our method accurately determines the different pixel-wise response functions. Hence, we can calibrate camera pictures taken from an LCD monitor to produce an output signal that is linear to the displayed brightness levels. Consequently, it permits the usage of continuous-tone or non-monochrome patterns displayed on the LCD monitor to calibrate a camera.

TABLE I. OVERALL MEASUREMENT OF THE ERRORS OF THE CALIBRATION PROCEDURE. SHOWN ARE THE MEAN ABSOLUTE ERROR AND THE MAXIMUM ABSOLUTE ERROR IN BRIGHTNESS LEVELS, THE LATTER WITH CORRESPONDING BRIGHTNESS LEVEL AT WHICH IT OCCURS. THE BEST SNR WITH THE RESPECTIVE BRIGHTNESS LEVEL AND THE OVERALL MEAN SNR ARE ALSO DISPLAYED. THE FIRST DATA ROW IS CALCULATED FOR FULL CAMERA RESOLUTION (1360 × 1024), THE SECOND ROW FOR THE CENTER REGION OF SIZE 1024 × 768.

| size | mean abs. error | max abs. error | at bright-ness | best SNR | at bright-ness | mean SNR |
|---|---|---|---|---|---|---|
| F | 1.16 | 2.66 | 254 | 46.47 | 223 | 40.17 |
| R | 0.91 | 1.81 | 254 | 48.16 | 223 | 42.14 |

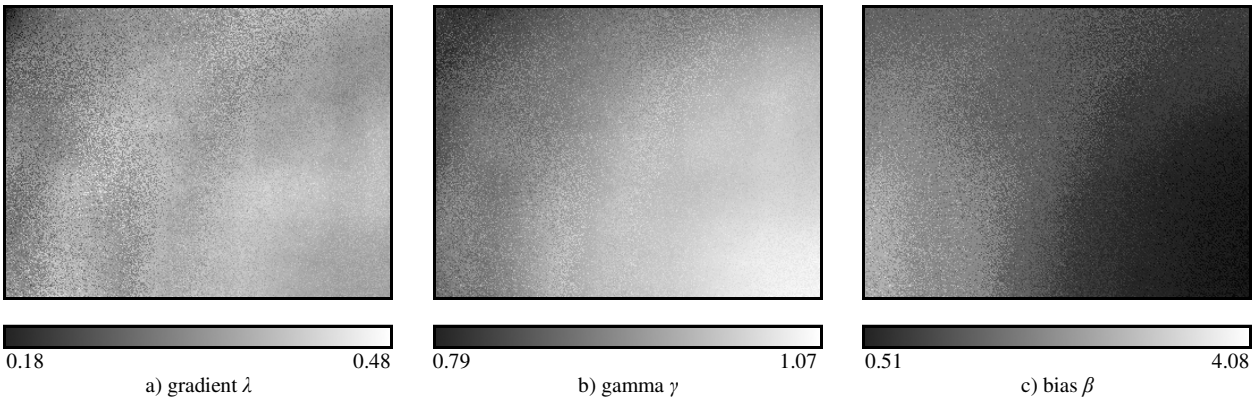


a) gradient $\lambda$ b) gamma $\gamma$ c) bias $\beta$

Figure 3. Estimated parameter $\lambda$, $\gamma$, and $\beta$ for all pixels of the upper left quarter of the red channel that minimize the error between Eq. (1) and the measured intensities for that pixel.

## CONCLUSION

We presented a method to estimate the composite monitor-camera response function for every single element of the camera target. The performed measurements in out setup showed that it is necessary to calibrate every pixel separately. An analysis of the calibration errors showed an overall error of under 0.45% of the displayed brightness levels, which corresponds to an SNR of 40.17 dB. These results show that the method is appropriate for calibration which permits camera calibration methods that are based on displaying calibration patterns on a monitor to use continuous-tone patterns.

## REFERENCES

[1] S. Lin and L. Zhang, "Determining the radiometric response function from a single grayscale image," in *Computer Vision and Pattern Recognition, IEEE Computer Society Conference on*, June 2005, vol. 2, pp. 66–73.

[2] S.J. Kim and M. Pollefeys, "Robust radiometric calibration and vignetting correction," *IEEE Transactions on Pattern Analysis and Machine Intelligence*, vol. 30, no. 4, April 2008.

[3] G.E. Healey and R. Kondepudy, "Radiometric ccd camera calibration and noise estimation," *IEEE Transactions on Pattern Analysis and Machine Intelligence*, vol. 16, no. 3, March 1994.

[4] T. Elbrandt, R. Dragon, and J. Ostermann, "Non-iterative camera calibration procedure using a virtual camera," in *Vision, Modeling, and Visualisation*, November 2007.

[5] R. Sagawa, M. Takatsuji, T. Echigo, and Y. Yagi, "Calibration of lens distortion by structured-light scanning," in *IEEE/RSJ International Conference on Intelligent Robots and Systems*, 2005, pp. 832–837.

[6] Paul E. Debevec and Jitendra Malik, "Recovering high dynamic range radiance maps from photographs," in *ACM SIGGRAPH*. 1997, pp. 369–378, ACM.

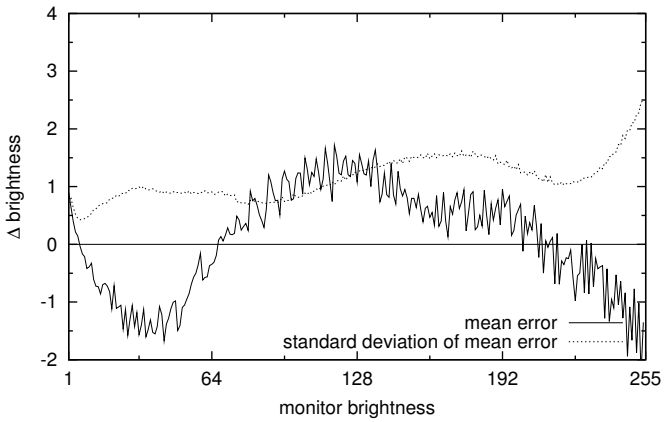


a) Mean error over brightness

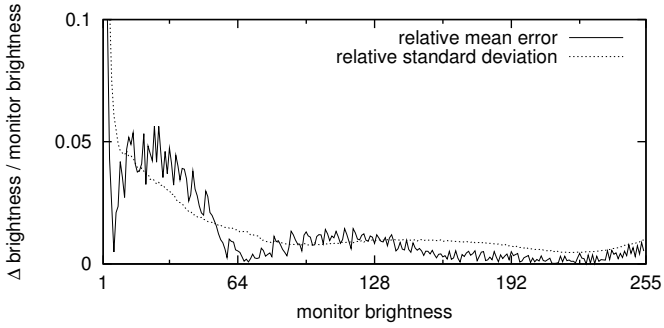


b) Absolute mean error and standard deviation relative to brightness

Figure 4. Differences between calibrated brightness and ground truth. a) shows the mean error and its standard deviation. b) shows the absolute mean error and the respective standard deviation in relation to the monitor brightness. The values are calculated for all calibrated pixels of the camera target.